Steel and Composite Structures, *Vol. 31, No. 4 (2019) 419-426*
DOI: https://doi.org/10.12989/scs.2019.31.4.419

Buckling analysis of plates reinforced by Graphene platelet based on Halpin-Tsai and Reddy theories

Rasool Javani, Mahmood Rabani Bidgoli* and Reza Kolahchi [a]

Department of Civil Engineering, Jasb Branch, Islamic Azad University, Jasb, Iran

(*Received December 25, 2018, Revised February 14, 2019, Accepted March 28, 2019*)

Abstract. In this paper, buckling analyses of composite plate reinforced by Graphen platelate (GPL) is studied. The Halphin-Tsai model is used for obtaining the effective material properties of nano composite plate. The nano composite plate is modeled by Third order shear deformation theory (TSDT). The elastic medium is simulated by Winkler model. Employing nonlinear strains-displacements, stress-strain, the energy equations of plate are obtained and using Hamilton's principal, the governing equations are derived. The governing equations are solved based on Navier method. The effect of GPL volume percent, geometrical parameters of plate and elastic foundation on the buckling load are investigated. Results showed that with increasing GPLs volume percent, the buckling load increases.

Keywords: buckling; nanocomposite plate; Graphen platelate; Reddy theory; Halphin-Tsai model

1. Introduction

Graphen platelate has many applications in different industries due to the high hardness-to-weight and strength-to-weight ratios and other better properties compared with traditional isotropic ones. These structures can be used in aircraft, helicopters, missiles, launchers, satellites and etc. During the last 5 decades the application of sandwich structures with light core and two thin factsheets have been extensively investigated.

A new sinusoidal shear deformation theory was developed by Thai and Vo (2013) for bending, buckling, and vibration of functionally graded plates. A simple refined shear deformation theory was proposed by Thai *et al*. (2013) for bending, buckling, and vibration of thick plates resting on elastic foundation. Forced vibration response of laminated composite and sandwich shell was studied by Kumar *et al*. (2014) using a 2D FE (finite element) model based on higher order zigzag theory (HOZT). The study of composite and nanocomposite paltes was presented by Duc *et al*. (Duc and Minh 2010, Duc *et al*. 2013, 2015, 2018). Chung *et al*. (2013) investigated Polymeric Composite Films Using Modified TiO2 Nanoparticles. Nonlocal dynamic buckling analysis of embedded micro plates reinforced by single-walled carbon nano tubes was studied by Kolahchi and Cheraghbak (2017). Wang *et al*. (2018) investigated buckling of functionally graded GPLs reinforced cylindrical shells consisting of multiple layers through FEM. Temperature-dependent buckling analysis of sandwich nano composite plates resting on elastic medium subjected to magnetic field was studied by Shokravi (2017). Li *et al*. (2018) investigated the static linear elasticity, natural frequency, and buckling behaviour of functionally graded porous plates reinforced by GPLs. GPL-reinforced titanium (Ti) composites (GPL/Ti) were prepared by Liu *et al*. (2018) using spark plasma sintering to evaluate a new type of structural material. Gao *et al*. (2018) studied free vibration of functionally graded (FG) porous nano composite plates reinforced with a small amount of GPLs and supported by the two-parameter elastic foundations with different boundary conditions. Polit *et al*. (2018) investigated thick functionally graded graphene platelets reinforced porous nano composite curved beams considering the static bending and elastic stability analyses based on a higher-order shear deformation theory accounting for through-thickness stretching effect. Transient dynamic analysis and elastic wave propagation in a functionally graded graphene platelets (FGGPLs)-reinforced composite thick hollow cylinder were presented by Hosseini and Zhang (2018). The in-plane and out-of-plane forced vibration of a curved nano composite micro beam were considered by Allahkarami *et al*. (2018). Vibration and nonlinear dynamic response of eccentrically stiffened functionally graded composite truncated conical shells in thermal environments were presented by Chan *et al*. (2018). Nonlinear response and buckling analysis of eccentrically stiffened FGM toroidal shell segments in thermal environment were studied by Vuong and Duc (2018). Large amplitude vibration problem of laminated composite spherical shell panel under combined temperature and moisture environment was analyzed by Mahapatra and Panda (2016). The nonlinear free vibration behaviour of laminated composite spherical shell panel under the elevated hygrothermal environment was investigated by Mahapatra and Panda (2016). Mahapatra *et al*. (2016b) studied the geometrically nonlinear transverse

*Corresponding author, Ph.D., Professor,
E-mail: m.rabanibidgoli@gmail.com
[a] Ph.D., Professor, E-mail: r.kolahchi@iaujasb.ac.ir

http://www.techno-press.org/?journal=scs&subpage=6
ISSN: 1229-9367 (Print), 1598-6233 (Online)

bending behavior of the shear deformable laminated composite spherical shell panel under hygro-thermo-mechanical loading. Nonlinear free vibration behavior of laminated composite curved panel under hygrothermal environment was investigated by Mahapatra *et al*. (2016c). The flexural behaviour of the laminated composite plate embedded with two different smart materials (piezoelectric and magnetostrictive) and subsequent deflection suppression were investigated by Dutta *et al*. (2017). Suman *et al*. (2017) studied static bending and strength behaviour of the laminated composite plate embedded with magnetostrictive (MS) material numerically using commercial finite element tool. Free vibration analyses of graphene reinforced singly and doubly curved laminated composite shell panels in thermal environment using finite element method were studied by Rout *et al*. (2019).

In this work, buckling analyses of composite plate reinforced by GPLs is studied. The Halphin-Tsai model is used for obtaining the effective material properties of nano composite plate. The nano composite plate is modeled by Third order shear deformation theory (TSDT). The elastic medium is simulated by Winkler model. Employing nonlinear strains-displacements, stress-strain, the energy equations of plate are obtained and using Hamilton's principal, the governing equations are derived. The governing equations are solved based on Navier method. The effect of GPL volume percent, geometrical parameters of plate and elastic foundation on the buckling load are investigated.

2. Kinematics of different theories

Fig. 1 shows a nanocomposite plate reinforced by GPLs resting on elastic medium.

Based on Third order shear deformation theory (TSDT), the orthogonal components of the displacement vector can be written as (Reddy 2002)

$$\begin{cases} u_1(x,y,z,t)=u(x,y,t)+z\,\phi_x(x,y,t) \\ +c_1 z^3\left(\phi_x+\dfrac{\partial w}{\partial x}\right), \\ u_2(x,y,z,t)=v(x,y,t)+z\,\phi_y(x,y,t) \\ +c_1 z^3\left(\phi_y+\dfrac{\partial w}{\partial y}\right), \\ u_3(x,y,z,t)=w(x,y,t), \end{cases} \tag{1}$$

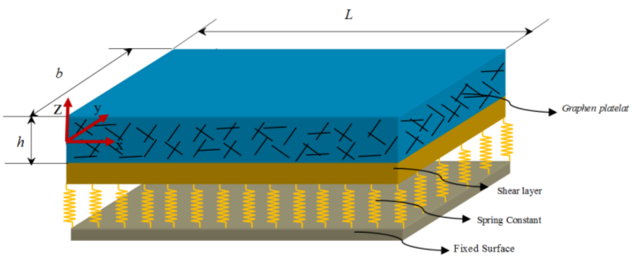

Fig. 1 A nanocomposite plate reinforced by GPLs resting on elastic medium

However, the strain–displacement relations can be given as

$$\begin{pmatrix}\varepsilon_{xx}\\ \varepsilon_{yy}\\ \gamma_{xy}\end{pmatrix}=\begin{pmatrix}\varepsilon_{xx}^0\\ \varepsilon_{yy}^0\\ \gamma_{xy}^0\end{pmatrix}+z\begin{pmatrix}\varepsilon_{xx}^1\\ \varepsilon_{yy}^1\\ \gamma_{xy}^1\end{pmatrix}+z^3\begin{pmatrix}\varepsilon_{xx}^3\\ \varepsilon_{yy}^3\\ \gamma_{xy}^3\end{pmatrix}, \tag{2}$$

$$\begin{pmatrix}\gamma_{yz}\\ \gamma_{xz}\end{pmatrix}=\begin{pmatrix}\gamma_{yz}^0\\ \gamma_{xz}^0\end{pmatrix}+z^2\begin{pmatrix}\gamma_{yz}^2\\ \gamma_{xz}^2\end{pmatrix}, \tag{3}$$

where

$$\begin{pmatrix}\varepsilon_{xx}^0\\ \varepsilon_{yy}^0\\ \gamma_{xy}^0\end{pmatrix}=\begin{pmatrix}\dfrac{\partial u}{\partial x}\\ \dfrac{\partial v}{\partial y}\\ \dfrac{\partial u}{\partial y}+\dfrac{\partial v}{\partial x}\end{pmatrix},\quad \begin{pmatrix}\varepsilon_{xx}^1\\ \varepsilon_{yy}^1\\ \gamma_{xy}^1\end{pmatrix}=\begin{pmatrix}\dfrac{\partial \varphi_x}{\partial x}\\ \dfrac{\partial \varphi_y}{\partial y}\\ \dfrac{\partial \varphi_x}{\partial y}+\dfrac{\partial \varphi_y}{\partial x}\end{pmatrix}$$
$$,\begin{pmatrix}\varepsilon_{xx}^3\\ \varepsilon_{yy}^3\\ \gamma_{xy}^3\end{pmatrix}=c_1\begin{pmatrix}\dfrac{\partial \varphi_x}{\partial x}+\dfrac{\partial^2 w}{\partial x^2}\\ \dfrac{\partial \varphi_y}{\partial y}+\dfrac{\partial^2 w}{\partial y^2}\\ \dfrac{\partial \varphi_x}{\partial y}+\dfrac{\partial \varphi_y}{\partial x}+2\dfrac{\partial^2 w}{\partial x\partial y}\end{pmatrix}, \tag{4}$$

$$\begin{pmatrix}\gamma_{yz}^0\\ \gamma_{xz}^0\end{pmatrix}=\begin{pmatrix}\phi_y+\dfrac{\partial w}{\partial y}\\ \phi_x+\dfrac{\partial w}{\partial x}\end{pmatrix},\quad \begin{pmatrix}\gamma_{yz}^2\\ \gamma_{xz}^2\end{pmatrix}=c_2\begin{pmatrix}\phi_y+\dfrac{\partial w}{\partial y}\\ \phi_x+\dfrac{\partial w}{\partial x}\end{pmatrix}, \tag{5}$$

where $c_2 = 3c_1$.

Hence, the strain-stress of this theory can be written as

$$\begin{bmatrix}\sigma_{xx}\\ \sigma_{yy}\\ \sigma_{zz}\\ \sigma_{zy}\\ \sigma_{xz}\\ \sigma_{zy}\end{bmatrix}=\begin{bmatrix}C_{11} & C_{12} & C_{13} & 0 & 0 & 0\\ C_{12} & C_{22} & C_{23} & 0 & 0 & 0\\ C_{13} & C_{23} & C_{33} & 0 & 0 & 0\\ 0 & 0 & 0 & C_{44} & 0 & 0\\ 0 & 0 & 0 & 0 & C_{55} & 0\\ 0 & 0 & 0 & 0 & 0 & C_{66}\end{bmatrix}\begin{bmatrix}\varepsilon_{xx}\\ \varepsilon_{yy}\\ \varepsilon_{zz}\\ \gamma_{zy}\\ \gamma_{xz}\\ \gamma_{xy}\end{bmatrix}, \tag{6}$$

where, parameters C_{ij} are elastic constant of composite plate where can be obtained by Halpin-Tsai micro mechanics model. Based on this model, we have (Halpin and Kardos 1976)

$$E_c=\frac{3*(1+\xi_l V_{GPL})}{8*(1-\eta_L V_{GPL})}*E_m+\frac{5*(1+\xi_W \eta_W V_{GPL})}{8*(1-\eta_W V_{GPL})}*E_m \tag{7}$$

where

$$\eta_L=\frac{\left(\dfrac{E_{GPL}}{E_M}\right)-1}{\left(\dfrac{E_{GPL}}{E_M}\right)+\xi_L} \tag{8}$$

$$\eta_W = \frac{\left(\frac{E_{GPL}}{E_M}\right)-1}{\left(\frac{E_{GPL}}{E_M}\right)+\eta_L} \tag{9}$$

and E_c, E_m, E_{GPL} are the effective Young's moduli of the GPL/polymer nano composite, polymer matrix, and GPLs, respectively. The effects of the geometry and size of GPL reinforcements are described through parameter.

$$\xi_L = 2\left(\frac{l_{GPL}}{h_{GPL}}\right); \tag{10}$$

$$\xi_W = 2\left(\frac{w_{GPL}}{h_{GPL}}\right) \tag{11}$$

in which l_{GPL}, w_{GPL} and h_{GPL} denote the length, width and thickness of the GPLs. The volume fraction of GPLs of the i-th layer can be obtained from GPL weight fraction fi and the mass densities of GPLs and polymer matrix, ρ_{GPL} and ρ_M, by

$$V_i = \frac{f_i}{f_i + \left(\frac{\rho_{GPL}}{\rho_M}\right)(1-f_i)} \tag{12}$$

3. Motion equation

For driving the motion equations, the Hamilton principle is used as follows

$$\delta U - \delta W = 0 \tag{13}$$

where δ is variation, δU is variation of potential energy and δW is variation of external work.

The variation of potential energy for composite plate can be written as

$$\mathrm{U} = \frac{1}{2}\int \begin{pmatrix} \sigma_{xx}\varepsilon_{xx} + \sigma_{yy}\varepsilon_{yy} + \sigma_{xy}\gamma_{xy} \\ +\sigma_{xz}\gamma_{xz} + \sigma_{yz}\gamma_{yz} \end{pmatrix} \mathrm{dV} \tag{14}$$

The variation of external work, due to elastic medium load simulated by Pasternak model can be express as

$$W_e = \iint \left(-K_w w + K_g \nabla^2 w\right) w dA, \tag{15}$$

Using the Hamilton principle and partial integral, the governing equations are computed as

Equation 1:

$$\delta u : \frac{\partial N_{xx}}{\partial x} + \frac{\partial N_{xy}}{\partial y} = 0, \tag{16}$$

Equation 2:

$$\delta v : \frac{\partial N_{xy}}{\partial x} + \frac{\partial N_{yy}}{\partial y} = 0, \tag{17}$$

Equation 3:

$$\begin{aligned} \delta w : &\frac{\partial Q_{xx}}{\partial x} + \frac{\partial Q_{yy}}{\partial y} + c_2\left(\frac{\partial K_{xx}}{\partial x} + \frac{\partial K_{yy}}{\partial y}\right) + N_{xx}\frac{\partial^2 w}{\partial x^2} + N_{yy}\frac{\partial^2 w}{\partial y^2} \\ &-c_1\left(\frac{\partial^2 P_{xx}}{\partial x^2} + 2\frac{\partial^2 P_{xy}}{\partial x\,\partial y} + \frac{\partial^2 P_{yy}}{\partial y^2}\right) - K_w w + K_g \nabla^2 w = 0 \end{aligned} \tag{18}$$

Equation 4:

$$\delta\phi_x : \frac{\partial M_{xx}}{\partial x} + \frac{\partial M_{xy}}{\partial y} + c_1\left(\frac{\partial P_{xx}}{\partial x} + \frac{\partial P_{xy}}{\partial y}\right) - Q_{xx} - c_2 K_{xx} = 0, \tag{19}$$

Equation 5:

$$\delta\phi_y : \frac{\partial M_{xy}}{\partial x} + \frac{\partial M_{yy}}{\partial y} + c_1\left(\frac{\partial P_{xy}}{\partial x} + \frac{\partial P_{yy}}{\partial y}\right) - Q_{yy} - c_2 K_{yy} = 0, \tag{20}$$

where, the force and moment resultants can be defined as

$$\begin{Bmatrix} N_{xx} \\ N_{yy} \\ N_{xy} \end{Bmatrix} = \int_{-h/2}^{h/2} \begin{bmatrix} \sigma_{xx} \\ \sigma_{yy} \\ \sigma_{xy} \end{bmatrix} dz, \tag{21}$$

$$\begin{Bmatrix} M_{xx} \\ M_{yy} \\ M_{xy} \end{Bmatrix} = \int_{-h/2}^{h/2} \begin{bmatrix} \sigma_{xx} \\ \sigma_{yy} \\ \sigma_{xy} \end{bmatrix} zdz, \tag{22}$$

$$\begin{Bmatrix} P_{xx} \\ P_{yy} \\ P_{xy} \end{Bmatrix} = \int_{-h/2}^{h/2} \begin{bmatrix} \sigma_{xx} \\ \sigma_{yy} \\ \sigma_{xy} \end{bmatrix} z^3 dz, \tag{23}$$

$$\begin{bmatrix} Q_{xx} \\ Q_{yy} \end{bmatrix} = \int_{-h/2}^{h/2} \begin{bmatrix} \sigma_{xz} \\ \sigma_{yz} \end{bmatrix} dz, \tag{24}$$

$$\begin{bmatrix} K_{xx} \\ K_{yy} \end{bmatrix} = \int_{-h/2}^{h/2} \begin{bmatrix} \sigma_{xz} \\ \sigma_{yz} \end{bmatrix} z^2 dz, \tag{25}$$

$$I_i = \int_{-h/2}^{h/2} \rho z^i dz \qquad (i = 0,1,\ldots,6), \tag{26}$$

$$J_i = I_i - \frac{4}{3h^2} I_{i+2} \qquad (i = 1,4), \tag{27}$$

$$K_2 = I_2 - \frac{8}{3h^2} I_4 + \left(\frac{4}{3h^2}\right)^2 I_6, \tag{28}$$

Therefore, the governing equations of nano composite plate can be written as

$$
\begin{aligned}
&A_{11}\frac{\partial^2 u}{\partial x^2}+A_{12}\frac{\partial^2 v}{\partial x\,\partial y}+A_{16}\left(\frac{\partial^2 u}{\partial x\,\partial y}+\frac{\partial^2 v}{\partial x^2}\right)+B_{11}\frac{\partial^2\varphi_x}{\partial x^2}\\
&+B_{12}\frac{\partial^2\varphi_y}{\partial x\,\partial y}+B_{16}\left(\frac{\partial^2\varphi_x}{\partial x\,\partial y}+\frac{\partial^2\varphi_y}{\partial x^2}\right)+E_{11}c_1\left(\frac{\partial^2\varphi_x}{\partial x^2}+\frac{\partial^3 w}{\partial x^3}\right)\\
&+E_{12}c_1\left(\frac{\partial^2\varphi_y}{\partial x\,\partial y}+\frac{\partial^3 w}{\partial x\,\partial y^2}\right)+E_{16}c_1\left(\frac{\partial^2\varphi_y}{\partial x^2}+\frac{\partial^2\varphi_x}{\partial x\,\partial y}+2\frac{\partial^3 w}{\partial x^2\partial y}\right)\\
&+A_{16}\frac{\partial^2 u}{\partial x\,\partial y}+A_{26}\frac{\partial^2 v}{\partial y^2}+A_{66}\left(\frac{\partial^2 u}{\partial y^2}+\frac{\partial^2 v}{\partial x\,\partial y}\right)+B_{16}\frac{\partial^2\varphi_x}{\partial x\,\partial y}\\
&+B_{26}\frac{\partial^2\varphi_y}{\partial y^2}+B_{66}\left(\frac{\partial^2\varphi_x}{\partial y^2}+\frac{\partial^2\varphi_y}{\partial x\,\partial y}\right)+E_{16}c_1\left(\frac{\partial^2\varphi_x}{\partial x\,\partial y}+\frac{\partial^3 w}{\partial y\,\partial x^2}\right)\\
&+E_{26}c_1\left(\frac{\partial^2\varphi_y}{\partial y^2}+\frac{\partial^3 w}{\partial y^3}\right)+E_{66}c_1\left(\frac{\partial^2\varphi_y}{\partial x\,\partial y}+\frac{\partial^2\varphi_x}{\partial y^2}+2\frac{\partial^3 w}{\partial x\,\partial y^2}\right)=0,
\end{aligned}
\tag{29}
$$

$$
\begin{aligned}
&A_{16}\frac{\partial^2 u}{\partial x^2}+A_{26}\frac{\partial^2 v}{\partial x\,\partial y}+A_{66}\left(\frac{\partial^2 u}{\partial x\,\partial y}+\frac{\partial^2 v}{\partial x^2}\right)+B_{16}\frac{\partial^2\varphi_x}{\partial x^2}\\
&+B_{26}\frac{\partial^2\varphi_y}{\partial x\,\partial y}+B_{66}\left(\frac{\partial^2\varphi_x}{\partial x\,\partial y}+\frac{\partial^2\varphi_y}{\partial x^2}\right)+E_{16}c_1\left(\frac{\partial^2\varphi_x}{\partial x^2}+\frac{\partial^3 w}{\partial x^3}\right)\\
&+E_{26}c_1\left(\frac{\partial^2\varphi_y}{\partial x\,\partial y}+\frac{\partial^3 w}{\partial x\,\partial y^2}\right)+E_{66}c_1\left(\frac{\partial^2\varphi_y}{\partial x^2}+\frac{\partial^2\varphi_x}{\partial x\,\partial y}+2\frac{\partial^3 w}{\partial x^2\partial y}\right)\\
&+A_{21}\frac{\partial^2 u}{\partial x\,\partial y}+A_{22}\frac{\partial^2 v}{\partial y^2}+A_{26}\left(\frac{\partial^2 u}{\partial y^2}+\frac{\partial^2 v}{\partial x\,\partial y}\right)+B_{21}\frac{\partial^2\varphi_x}{\partial x\,\partial y}\\
&+B_{22}\frac{\partial^2\varphi_y}{\partial y^2}+B_{26}\left(\frac{\partial^2\varphi_x}{\partial y^2}+\frac{\partial^2\varphi_y}{\partial x\,\partial y}\right)+E_{21}c_1\left(\frac{\partial^2\varphi_x}{\partial x\,\partial y}+\frac{\partial^3 w}{\partial y\,\partial x^2}\right)\\
&+E_{22}c_1\left(\frac{\partial^2\varphi_y}{\partial y^2}+\frac{\partial^3 w}{\partial y^3}\right)+E_{26}c_1\left(\frac{\partial^2\varphi_y}{\partial x\,\partial y}+\frac{\partial^2\varphi_x}{\partial y^2}+2\frac{\partial^3 w}{\partial x\,\partial y^2}\right)=0,
\end{aligned}
\tag{30}
$$

$$
\begin{aligned}
&A_{55}\left(\frac{\partial^2 w}{\partial x^2}+\frac{\partial\varphi_x}{\partial x}\right)+A_{45}\left(\frac{\partial^2 w}{\partial x\,\partial y}+\frac{\partial\varphi_y}{\partial x}\right)+D_{55}c_2\left(\frac{\partial^2 w}{\partial x^2}+\frac{\partial\varphi_x}{\partial x}\right)\\
&+D_{45}c_2\left(\frac{\partial^2 w}{\partial x\,\partial y}+\frac{\partial\varphi_y}{\partial x}\right)+A_{45}\left(\frac{\partial^2 w}{\partial x\,\partial y}+\frac{\partial\varphi_x}{\partial y}\right)+A_{44}\left(\frac{\partial^2 w}{\partial y^2}+\frac{\partial\varphi_y}{\partial y}\right)\\
&+D_{45}c_2\left(\frac{\partial^2 w}{\partial x\,\partial y}+\frac{\partial\varphi_x}{\partial y}\right)+D_{44}c_2\left(\frac{\partial^2 w}{\partial y^2}+\frac{\partial\varphi_y}{\partial y}\right)\\
&+c_2\left|\begin{matrix}D_{55}\left(\frac{\partial^2 w}{\partial x^2}+\frac{\partial\varphi_x}{\partial x}\right)+D_{45}\left(\frac{\partial^2 w}{\partial x\,\partial y}+\frac{\partial\varphi_y}{\partial x}\right)+F_{55}c_2\left(\frac{\partial^2 w}{\partial x^2}+\frac{\partial\varphi_x}{\partial x}\right)\\
+F_{45}c_2\left(\frac{\partial^2 w}{\partial x\,\partial y}+\frac{\partial\varphi_y}{\partial x}\right)+D_{45}\left(\frac{\partial^2 w}{\partial x\,\partial y}+\frac{\partial\varphi_x}{\partial y}\right)+D_{44}\left(\frac{\partial^2 w}{\partial y^2}+\frac{\partial\varphi_y}{\partial y}\right)\\
+F_{45}c_2\left(\frac{\partial^2 w}{\partial x\,\partial y}+\frac{\partial\varphi_x}{\partial y}\right)+F_{44}c_2\left(\frac{\partial^2 w}{\partial y^2}+\frac{\partial\varphi_y}{\partial y}\right)\end{matrix}\right|\\
&+-K_w w+K_g\nabla^2 w-c_1\bigg(E_{11}\frac{\partial^3 u}{\partial x^3}+E_{12}\frac{\partial^3 v}{\partial x^2\partial y}+E_{16}\left(\frac{\partial^3 u}{\partial x^2\partial y}+\frac{\partial^3 v}{\partial x^3}\right)\\
&+F_{11}\frac{\partial^3\varphi_x}{\partial x^3}+F_{12}\frac{\partial^3\varphi_y}{\partial x^2\partial y}+F_{16}\left(\frac{\partial^3\varphi_x}{\partial x^2\partial y}+\frac{\partial^3\varphi_y}{\partial x^3}\right)+H_{11}c_1\left(\frac{\partial^3\varphi_x}{\partial x^3}+\frac{\partial^4 w}{\partial x^4}\right)\\
&+H_{12}c_1\left(\frac{\partial^3\varphi_y}{\partial x^2\partial y}+\frac{\partial^4 w}{\partial x^2\partial y^2}\right)+H_{16}c_1\left(\frac{\partial^3\varphi_y}{\partial x^3}+\frac{\partial^3\varphi_x}{\partial x^2\partial y}+2\frac{\partial^4 w}{\partial x^3\partial y}\right)\\
&+E_{12}\frac{\partial^3 u}{\partial y^2\partial x}+E_{22}\frac{\partial^3 v}{\partial y^3}+E_{26}\left(\frac{\partial^3 u}{\partial y^3}+\frac{\partial^3 v}{\partial x\,\partial y^2}\right)
\end{aligned}
\tag{31}
$$

$$
\begin{aligned}
&+F_{12}\frac{\partial^3\varphi_x}{\partial x\,\partial y^2}+F_{22}\frac{\partial^3\varphi_y}{\partial y^3}+F_{26}\left(\frac{\partial^3\varphi_x}{\partial y^3}+\frac{\partial^3\varphi_y}{\partial x\,\partial y^2}\right)\\
&+H_{12}c_1\left(\frac{\partial^3\varphi_x}{\partial x\,\partial y^2}+\frac{\partial^4 w}{\partial x^2\partial y^2}\right)+H_{22}c_1\left(\frac{\partial^3\varphi_y}{\partial y^3}+\frac{\partial^4 w}{\partial y^4}\right)\\
&+H_{26}c_1\left(\frac{\partial^3\varphi_y}{\partial x\,\partial y^2}+\frac{\partial^3\varphi_x}{\partial y^3}+2\frac{\partial^4 w}{\partial x\,\partial y^3}\right)+2E_{16}\frac{\partial^3 u}{\partial y\,\partial x^2}+2E_{26}\frac{\partial^3 v}{\partial y^2\partial x}\\
&+2E_{66}\left(\frac{\partial^3 u}{\partial y^2\partial x}+\frac{\partial^3 v}{\partial x^2\partial y}\right)+2F_{16}\frac{\partial^3\varphi_x}{\partial x^2\partial y}+2F_{26}\frac{\partial^3\varphi_y}{\partial y^2\partial x}\\
&+2F_{66}\left(\frac{\partial^3\varphi_x}{\partial y^2\partial x}+\frac{\partial^3\varphi_y}{\partial x^2\partial y}\right)+2H_{16}c_1\left(\frac{\partial^3\varphi_x}{\partial x^2\partial y}+\frac{\partial^4 w}{\partial x^3\partial y}\right)\\
&+2H_{26}c_1\left(\frac{\partial^3\varphi_y}{\partial x\,\partial y^2}+\frac{\partial^4 w}{\partial y^3\partial x}\right)+2H_{66}c_1\left(\frac{\partial^3\varphi_y}{\partial x^2\partial y}+\frac{\partial^3\varphi_x}{\partial y^2\partial x}+2\frac{\partial^4 w}{\partial x^2\partial y^2}\right)\\
&+N_{xx}\frac{\partial^2 w}{\partial x^2}+N_{yy}\frac{\partial^2 w}{\partial y^2}=0,
\end{aligned}
\tag{31}
$$

$$
\begin{aligned}
&B_{11}\frac{\partial^2 u}{\partial x^2}+B_{12}\frac{\partial^2 v}{\partial x\,\partial y}+B_{16}\left(\frac{\partial^2 u}{\partial x\,\partial y}+\frac{\partial^2 v}{\partial x^2}\right)+D_{11}\frac{\partial^2\varphi_x}{\partial x^2}\\
&+D_{12}\frac{\partial^2\varphi_y}{\partial x\,\partial y}+D_{16}\left(\frac{\partial^2\varphi_x}{\partial x\,\partial y}+\frac{\partial^2\varphi_y}{\partial x^2}\right)+F_{11}c_1\left(\frac{\partial^2\varphi_x}{\partial x^2}+\frac{\partial^3 w}{\partial x^3}\right)\\
&+F_{12}c_1\left(\frac{\partial^2\varphi_y}{\partial x\,\partial y}+\frac{\partial^3 w}{\partial x\,\partial y^2}\right)+F_{16}c_1\left(\frac{\partial^2\varphi_y}{\partial x^2}+\frac{\partial^2\varphi_x}{\partial x\,\partial y}+2\frac{\partial^3 w}{\partial x^2\partial y}\right)\\
&+B_{16}\frac{\partial^2 u}{\partial x\,\partial y}+B_{26}\frac{\partial^2 v}{\partial y^2}+B_{66}\left(\frac{\partial^2 u}{\partial y^2}+\frac{\partial^2 v}{\partial x\,\partial y}\right)+D_{16}\frac{\partial^2\varphi_x}{\partial x\,\partial y}\\
&+D_{26}\frac{\partial^2\varphi_y}{\partial y^2}+D_{66}\left(\frac{\partial^2\varphi_x}{\partial y^2}+\frac{\partial^2\varphi_y}{\partial x\,\partial y}\right)+F_{16}c_1\left(\frac{\partial^2\varphi_x}{\partial x\,\partial y}+\frac{\partial^3 w}{\partial y\,\partial x^2}\right)\\
&+F_{26}c_1\left(\frac{\partial^2\varphi_y}{\partial y^2}+\frac{\partial^3 w}{\partial y^3}\right)+F_{66}c_1\left(\frac{\partial^2\varphi_y}{\partial x\,\partial y}+\frac{\partial^2\varphi_x}{\partial y^2}+2\frac{\partial^3 w}{\partial x\,\partial y^2}\right)\\
&+c_1\bigg(E_{11}\frac{\partial^2 u}{\partial x^2}+E_{12}\frac{\partial^2 v}{\partial x\,\partial y}+E_{16}\left(\frac{\partial^2 u}{\partial x\,\partial y}+\frac{\partial^2 v}{\partial x^2}\right)\\
&+F_{11}\frac{\partial^2\varphi_x}{\partial x^2}+F_{12}\frac{\partial^2\varphi_y}{\partial x\,\partial y}+F_{16}\left(\frac{\partial^2\varphi_x}{\partial x\,\partial y}+\frac{\partial^2\varphi_y}{\partial x^2}\right)\\
&+H_{11}c_1\left(\frac{\partial^2\varphi_x}{\partial x^2}+\frac{\partial^3 w}{\partial x^3}\right)+H_{12}c_1\left(\frac{\partial^2\varphi_y}{\partial x\,\partial y}+\frac{\partial^3 w}{\partial x\,\partial y^2}\right)\\
&+H_{16}c_1\left(\frac{\partial^2\varphi_y}{\partial x^2}+\frac{\partial^2\varphi_x}{\partial x\,\partial y}+2\frac{\partial^3 w}{\partial x^2\partial y}\right)+E_{16}\frac{\partial^2 u}{\partial x\,\partial y}+E_{26}\frac{\partial^2 v}{\partial y^2}\\
&+E_{66}\left(\frac{\partial^2 u}{\partial y^2}+\frac{\partial^2 v}{\partial x\,\partial y}\right)+F_{16}\frac{\partial^2\varphi_x}{\partial x\,\partial y}+F_{26}\frac{\partial^2\varphi_y}{\partial y^2}+F_{66}\left(\frac{\partial^2\varphi_x}{\partial y^2}+\frac{\partial^2\varphi_y}{\partial x\,\partial y}\right)\\
&+H_{16}c_1\left(\frac{\partial^2\varphi_x}{\partial x\,\partial y}+\frac{\partial^3 w}{\partial y\,\partial x^2}\right)+H_{26}c_1\left(\frac{\partial^2\varphi_y}{\partial y^2}+\frac{\partial^3 w}{\partial y^3}\right)\\
&+H_{66}c_1\left(\frac{\partial^2\varphi_y}{\partial x\,\partial y}+\frac{\partial^2\varphi_x}{\partial y^2}+2\frac{\partial^3 w}{\partial x\,\partial y^2}\right)-A_{55}\left(\frac{\partial w}{\partial x}+\varphi_x\right)-A_{45}\left(\frac{\partial w}{\partial y}+\varphi_y\right)\\
&-D_{55}c_2\left(\varphi_x+\frac{\partial w}{\partial x}\right)-D_{45}c_2\left(\frac{\partial w}{\partial y}+\varphi_y\right)\\
&+c_2\left|\begin{matrix}-D_{55}\left(\frac{\partial w}{\partial x}+\varphi_x\right)-D_{45}\left(\frac{\partial w}{\partial y}+\varphi_y\right)\\
-F_{55}c_2\left(\varphi_x+\frac{\partial w}{\partial x}\right)-F_{45}c_2\left(\frac{\partial w}{\partial y}+\varphi_y\right)\end{matrix}\right|=0,
\end{aligned}
\tag{32}
$$

$$
\begin{aligned}
&B_{16}\frac{\partial^2 u}{\partial x^2}+B_{26}\frac{\partial^2 v}{\partial x\,\partial y}+B_{66}\left(\frac{\partial^2 u}{\partial x\,\partial y}+\frac{\partial^2 v}{\partial x^2}\right)+D_{16}\frac{\partial^2\varphi_x}{\partial x^2}\\
&+D_{26}\frac{\partial^2\varphi_y}{\partial x\,\partial y}+D_{66}\left(\frac{\partial^2\varphi_x}{\partial x\,\partial y}+\frac{\partial^2\varphi_y}{\partial x^2}\right)+F_{16}c_1\left(\frac{\partial^2\varphi_x}{\partial x^2}+\frac{\partial^3 w}{\partial x^3}\right)
\end{aligned}
\tag{33}
$$

$$
\begin{aligned}
&+F_{26}c_1\left(\frac{\partial^2\varphi_y}{\partial x\,\partial y}+\frac{\partial^3 w}{\partial x\,\partial y^2}\right)+F_{66}c_1\left(\frac{\partial^2\varphi_y}{\partial x^2}+\frac{\partial^2\varphi_x}{\partial x\,\partial y}+2\frac{\partial^3 w}{\partial x^2\partial y}\right)\\
&+B_{12}\frac{\partial^2 u}{\partial x\,\partial y}+B_{22}\frac{\partial^2 v}{\partial y^2}+B_{26}\left(\frac{\partial^2 u}{\partial y^2}+\frac{\partial^2 v}{\partial x\,\partial y}\right)+D_{12}\frac{\partial^2\varphi_x}{\partial x\,\partial y}\\
&+D_{22}\frac{\partial^2\varphi_y}{\partial y^2}+D_{26}\left(\frac{\partial^2\varphi_x}{\partial y^2}+\frac{\partial^2\varphi_y}{\partial x\,\partial y}\right)+F_{12}c_1\left(\frac{\partial^2\varphi_x}{\partial x\,\partial y}+\frac{\partial^3 w}{\partial y\,\partial x^2}\right)\\
&+F_{22}c_1\left(\frac{\partial^2\varphi_y}{\partial y^2}+\frac{\partial^3 w}{\partial y^3}\right)+F_{26}c_1\left(\frac{\partial^2\varphi_y}{\partial x\,\partial y}+\frac{\partial^2\varphi_x}{\partial y^2}+2\frac{\partial^3 w}{\partial x\,\partial y^2}\right)\\
&+c_1\left(E_{16}\frac{\partial^2 u}{\partial x^2}+E_{26}\frac{\partial^2 v}{\partial x\,\partial y}+E_{66}\left(\frac{\partial^2 u}{\partial x\,\partial y}+\frac{\partial^2 v}{\partial x^2}\right)\right.\\
&+F_{16}\frac{\partial^2\varphi_x}{\partial x^2}+F_{26}\frac{\partial^2\varphi_y}{\partial x\,\partial y}+F_{66}\left(\frac{\partial^2\varphi_x}{\partial x\,\partial y}+\frac{\partial^2\varphi_y}{\partial x^2}\right)+H_{16}c_1\left(\frac{\partial^2\varphi_x}{\partial x^2}+\frac{\partial^3 w}{\partial x^3}\right)\\
&+H_{26}c_1\left(\frac{\partial^2\varphi_y}{\partial x\,\partial y}+\frac{\partial^3 w}{\partial x\,\partial y^2}\right)+H_{66}c_1\left(\frac{\partial^2\varphi_y}{\partial x^2}+\frac{\partial^2\varphi_x}{\partial x\,\partial y}+2\frac{\partial^3 w}{\partial x^2\partial y}\right)\\
&+E_{12}\frac{\partial^2 u}{\partial x\,\partial y}+E_{22}\frac{\partial^2 v}{\partial y^2}+E_{26}\left(\frac{\partial^2 u}{\partial y^2}+\frac{\partial^2 v}{\partial x\,\partial y}\right)+F_{12}\frac{\partial^2\varphi_x}{\partial x\,\partial y}+F_{22}\frac{\partial^2\varphi_y}{\partial y^2}\\
&+F_{26}\left(\frac{\partial^2\varphi_x}{\partial y^2}+\frac{\partial^2\varphi_y}{\partial x\,\partial y}\right)+H_{12}c_1\left(\frac{\partial^2\varphi_x}{\partial x\,\partial y}+\frac{\partial^3 w}{\partial y\,\partial x^2}\right)+H_{22}c_1\left(\frac{\partial^2\varphi_y}{\partial y^2}+\frac{\partial^3 w}{\partial y^3}\right)\\
&+H_{26}c_1\left(\frac{\partial^2\varphi_y}{\partial x\,\partial y}+\frac{\partial^2\varphi_x}{\partial y^2}+2\frac{\partial^3 w}{\partial x\,\partial y^2}\right)-A_{45}\left(\frac{\partial w}{\partial x}+\varphi_x\right)-A_{44}\left(\frac{\partial w}{\partial y}+\varphi_y\right)\\
&-D_{45}c_2\left(\varphi_x+\frac{\partial w}{\partial x}\right)-D_{44}c_2\left(\frac{\partial w}{\partial y}+\varphi_y\right)\\
&+c_2\left(\begin{array}{l}-D_{45}\left(\dfrac{\partial w}{\partial x}+\varphi_x\right)-D_{44}\left(\dfrac{\partial w}{\partial y}+\varphi_y\right)\\ -F_{45}c_2\left(\varphi_x+\dfrac{\partial w}{\partial x}\right)-F_{44}c_2\left(\dfrac{\partial w}{\partial y}+\varphi_y\right)\end{array}\right)=0,
\end{aligned}
\tag{33}
$$

where

$$A_{ij}=\int_{-h/2}^{h/2}Q_{ij}dz, \qquad (i,j=1,2,6) \tag{34}$$

$$B_{ij}=\int_{-h/2}^{h/2}Q_{ij}z\,dz, \tag{35}$$

$$D_{ij}=\int_{-h/2}^{h/2}Q_{ij}z^2dz, \tag{36}$$

$$E_{ij}=\int_{-h/2}^{h/2}Q_{ij}z^3dz, \tag{37}$$

$$F_{ij}=\int_{-h/2}^{h/2}Q_{ij}z^4dz, \tag{38}$$

$$H_{ij}=\int_{-h/2}^{h/2}Q_{ij}z^6dz, \tag{39}$$

4. Solution method

Base on Navier method, the displacements of the composite plate with simply supported boundary condition can be written as

$$u(x,y,t)=u_0\cos\left(\frac{n\pi x}{L}\right)\sin\left(\frac{m\pi y}{b}\right)e^{i\omega t}, \tag{40}$$

$$v(x,y,t)=v_0\sin\left(\frac{n\pi x}{L}\right)\cos\left(\frac{m\pi y}{b}\right)e^{i\omega t}, \tag{41}$$

$$w(x,y,t)=w_0\sin\left(\frac{n\pi x}{L}\right)\sin\left(\frac{m\pi y}{b}\right)e^{i\omega t}, \tag{42}$$

$$\phi_x(x,y,t)=\psi_{x0}\cos\left(\frac{n\pi x}{L}\right)\sin\left(\frac{m\pi y}{b}\right)e^{i\omega t}, \tag{43}$$

$$\phi_y(x,y,t)=\psi_{y0}\sin\left(\frac{n\pi x}{L}\right)\cos\left(\frac{m\pi y}{b}\right)e^{i\omega t}, \tag{44}$$

where, n is vibration mode number and ω is frequency. Substituting Eqs. (40)-(44) into Eqs. (29)-(33), the motion equations in matrix form can be expressed as

$$[K]\begin{bmatrix}u_0\\ v_0\\ w_0\\ \psi_{x0}\\ \psi_{y0}\end{bmatrix}=0, \tag{45}$$

where $[k_{ij}]$ is stiffness matrix.

4. Numerical result and discussion

In this section, a parametric study is done for the effects of different parameters on the nonlinear buckling load of the composite structure.

Figs. 2 and 3 show the effect of different transverse to axial lode ratio and plate width on the buckling load versus mode number, respectively. As it is inferred with increasing transverse to axial lode ratio and plate width, the buckling load has reduction**.** It is because with increasing transverse to axial lode ratio and plate width, stiffness of system is decreased. In addition, increasing mode number, buckling load is increased.

Fig. 4 illustrates the effect of plate thickness on the buckling lode versus mode number. It can be concluded with plate thickness increases, stiffness of system is

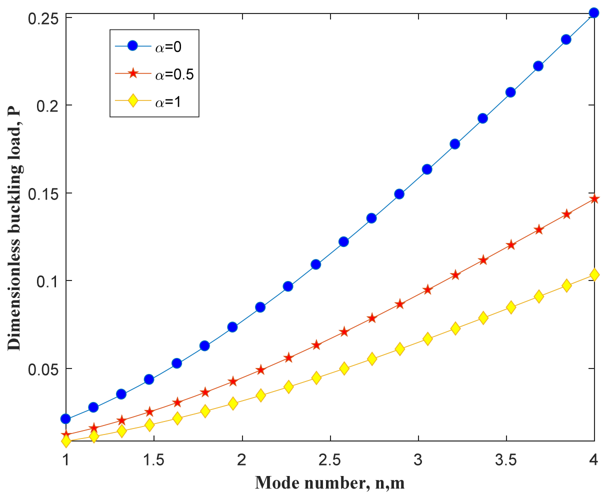

Fig. 2 Dimensionless buckling load versus mode number for different transverse to axial lode ratio

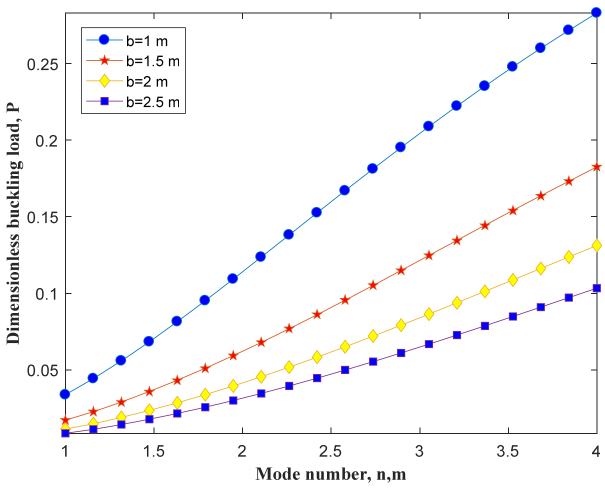

Fig. 3 The effect of plate width on the dimensionless buckling load versus mode number

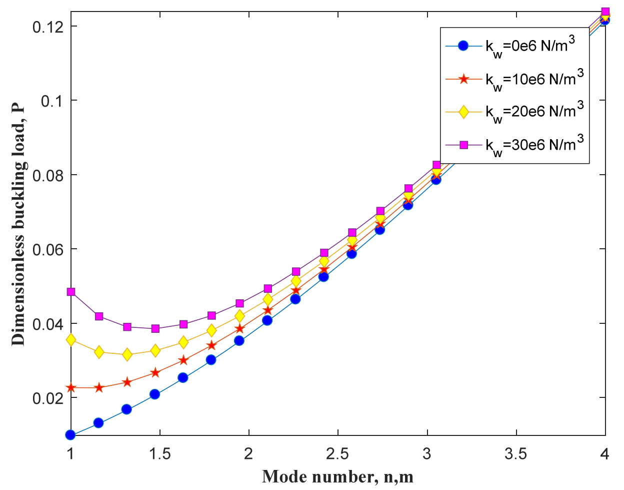

Fig. 5 The effect of spring constant of elastic medium on the dimensionless buckling load versus mode number

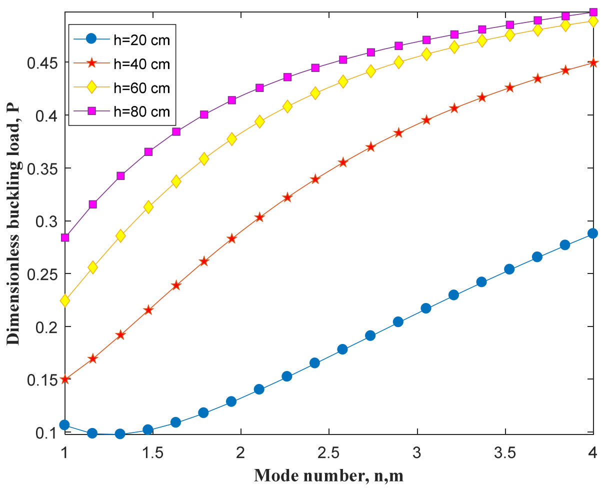

Fig. 4 The effect plate thickens on the dimensionless buckling load versus mode number

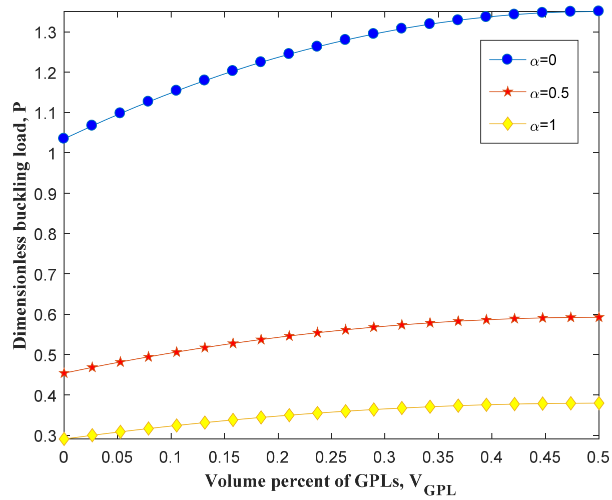

Fig. 6 The effect of plate length on the dimensionless buckling load versus mode number

increased. It is because the buckling load is increased.

Fig. 5 indicates the effect of spring constant of elastic medium on the buckling load with respect to mode number. It is observed that with increasing spring constant of elastic medium, the buckling load is increased. It is because stiffness of system is increased with enhancing spring constant of elastic medium.

The effect of plate length on the buckling load as function of mode number is shown in Fig. 6. With increasing plate length, buckling load decreases. It is because stiffness of structure is decreased.

Fig. 7 shows buckling load versus volume present of GPL for different transverse to axial lode ratio. As can be seen, the buckling load of micro composite structure with increasing transverse to axial lode ratio is decreased. Furthermore, with increasing the GPL volume percent, the buckling load is increased due to increase in the bending rigidity of the structure.The effect of volume percent of GPLs on the buckling load is shown in Fig. 8 for different length to thickness ratio of the GPLs (zeta). It is found that with increasing the zeta, the buckling load is decreased

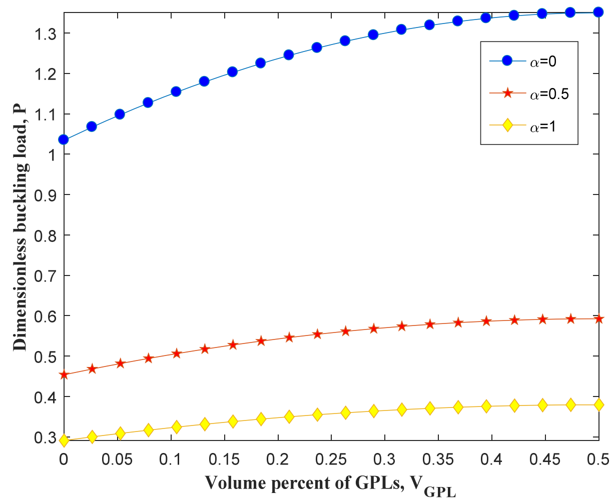

Fig. 7 Dimensionless buckling load versus volume percent of GPLs for different transverse to axial lode ratio

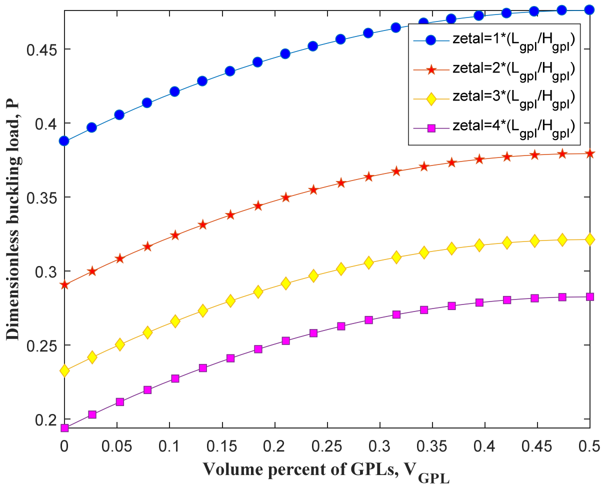

Fig. 8 The effect of volume percent of GPLs on the dimensionless buckling load for different length to thickness ratio of the GPLs

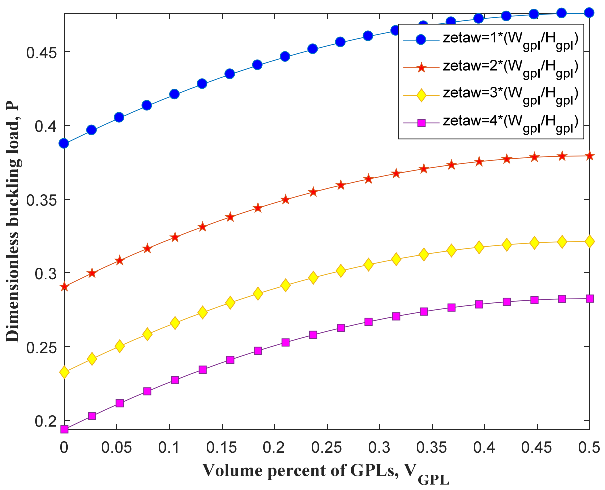

Fig. 9 The effect of weight to thickness ratio of GPLs on the buckling load versus volume percent of GPLs

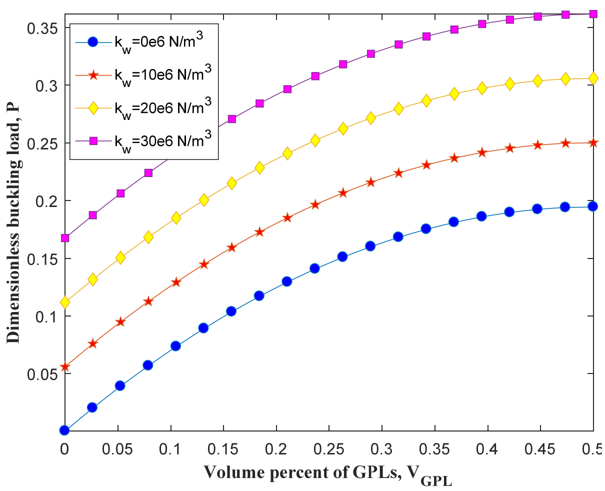

Fig. 10 The effect of spring constant of elastic medium on the buckling load versus volume percent of GPLs

due to the enhance in the stiffness of the structure.

Fig. 9 shows the effect of weight to thickness ratio of GPLs (zetaw) on the buckling load versus volume percent of GPLs. As can be seen, with increasing zetaw, the buckling load is decreased. It is since with increasing zetaw, the stiffness is decreased.

Fig. 10 indicates the effect of spring constant of elastic medium on the buckling load with respect to volume percent of GPLs. It is observed that with increasing spring constant of elastic medium, the buckling load is increased. It is because stiffness of system is increased with enhancing spring constant of elastic medium.

5. Conclusions

In this work, buckling analyses of composite plate reinforced by GPL restiong on elastic medium was presented. The elastic medium was simulated by Winkler model. The Halpin-Tsai model for considering effect of GPLs was used. The motion equations were calculated by TSDT, Hamilton's principle and energy method. Using analytical method, the buckling load of the structure was obtained. The effect of GPL volume percent, geometrical parameters of plate and elastic foundation on the buckling load were investigated. Increasing volume percent of GPLs, buckling load was increased. Increasing spring constant of elastic medium, the buckling load was increased. In addition, with increasing zeta, buckling lode decreases.

References

Allahkarami, F., Nikkhah-bahrami, M. and Ghassabzadeh Saryazdi, M. (2018), "Nonlinear forced vibration of FG-CNTs-reinforced curved microbeam based on strain gradient theory considering out-of-plane motion", *Steel Compos. Struct., Int. J.*, **22**(6), 673-691.

Chan, D.Q., Anh, V.T.T. and Duc, N.D. (2018), "Vibration and nonlinear dynamic response of eccentrically stiffened functionally graded composite truncated conical shells in thermal environments", *Acta Mech.*, **230**, 157-178.

Chung, D.N., Dinh, N.N., Hui, D., Duc, N.D., Trung, T.Q. and Chipara, M. (2013), "Investigation of Polymeric Composite Films Using Modified TiO2 Nanoparticles for Organic Light Emitting Diodes", *J. Current Nanosci.*, **9**, 14-20.

Duc, N.D. (2014a), *Nonlinear Static and Dynamic Stability of Functionally Graded Plates and Shells*, Vietnam National University Press, Hanoi, Vietnam.

Duc, N.D. (2014b), "Nonlinear dynamic response of imperfect eccentrically stiffened FGM double curved shallow shells on elastic foundation", *J. Compos. Struct.*, **102**, 306-314.

Duc, N.D. (2016), "Nonlinear thermal dynamic analysis of eccentrically stiffened S-FGM circular cylindrical shells surrounded on elastic foundations using the Reddy's third-order shear deformation shell theory", *Eur. J. Mech. – A/Solids*, **58**, 10-30.

Duc, N.D. and Minh, D.K. (2010), "Bending analysis of three-phase polymer composite plates reinforced by glass fibers and Titanium oxide particles", *J. Computat. Mat. Sci.*, **49**, 194-198.

Duc, N.D., Quan, T.Q. and Nam, D. (2013), "Nonlinear stability analysis of imperfect three phase polymer composite plates", *J. Mech. Compos. Mat.*,**49**, 345-358.

Duc, N.D., Hadavinia, H., Thu, P.V. and Quan, T.Q. (2015), "Vibration and nonlinear dynamic response of imperfect three-phase polymer nanocomposite panel resting on elastic foundations under hydrodynamic loads", *Compos. Struct.*, **131**, 229-237.

Duc, N.D., Khoa, N.D. and Thiem, H.T. (2018), "Nonlinear thermo-mechanical response of eccentrically stiffened Sigmoid FGM circular cylindrical shells subjected to compressive and uniform radial loads using the Reddy's third-order shear deformation shell theory", *Mech. Adv. Mat. Struct.*, **25**, 1157-1167.

Dutta, G., Panda. S.K., Mahapatra, T.R. and Singh, V.K. (2017), "Electro-magneto-elastic response of laminated composite plate: A finite element approach", *Int. J. Appl. Computat. Math.*, **3**, 2573-2592.

Gao, K., Gao, W., Chen, D. and Yang, J. (2018), "Nonlinear free vibration of functionally graded graphene concrete platelets reinforced porous nano composite concrete plates resting on elastic foundation", *Compos. Struct.*, **204**, 831-846.

Halpin, J.C. and Kardos, J.L. (1976), "The Halpin-Tsai equations: a review", *Polym. Eng. Sci.*, **16**(5), 344-352.

Hosseini, S.M. and Zhang, Ch. (2018), "Elastodynamic and wave propagation analysis in a FG graphene platelets-reinforced nanocomposite cylinder using a modified nonlinear micromechanical model", *Steel Compos. Struct.*, *Int. J.*, **27**(3), 255-271.

Kolahchi, R. and Cheraghbak, A. (2017), "Agglomeration effects on the dynamic buckling of visco elastic micro concrete plates reinforced with SWCNTs using Bolotin method", *Nonlin. Dynam.*, **90**, 479-492

Kumar, A., Chakrabarti, A. and Bhargava, P. (2014), "Accurate dynamic response of laminated composites and sandwich shells using higher order zigzag theory", *Thin-Wall. Struct.*, **77**, 174-186.

Li, K., Wu, D., Chen X., Cheng J., Liu Zh., Gao, W. and Liu, M. (2018), "Isogeometric Analysis of functionally graded porous concrete plates reinforced by graphene concrete platelets", *Compos. Struct.*, **204**, 114-130.

Liu, J., Wu, M., Yang, Y., Yang, G., Yan, H. and Jiang, K. (2018), "Preparation and mechanical performance of graphene concrete platelet reinforced titanium nanocomposites for high temperature applications", *J. Alloys Compounds*, **765**, 1111-1118.

Mahapatra, T.R. and Panda, S.K. (2016), "Nonlinear free vibration analysis of laminated composite spherical shell panel under elevated hygrothermal environment: A micromechanical approach", *Aerosp. Sci. Technol.*, **49**, 276-288.

Mahapatra, T.R., Panda, S.K. and Kar, V.R. (2016a), "Nonlinear flexural analysis of laminated composite panel under hygro-thermo-mechanical loading—A micromechanical approach", *Int. J. Computat. Meth.*, **13**, 1650015.

Mahapatra, T.R., Panda, S.K. and Kar, V.R. (2016b), "Nonlinear hygro-thermo-elastic vibration analysis of doubly curved composite shell panel using finite element micromechanical model", *Mech. Advan. Mat. Struct.*, **23**, 1343-1359.

Mahapatra, T.R., Panda, S.K. and Kar, V.R. (2016c), "Geometrically nonlinear flexural analysis of hygro-thermo-elastic laminated composite doubly curved shell panel", *Int. J. Mech. Mat. Des.*, **12**, 153-171.

Mahi, A., Bedia, E.A.A. and Tounsi, A. (2015), "A new hyperbolic shear deformation theory for bending and free vibration analysis of isotropic, functionally graded, sandwich and laminated composite plates", *Appl. Math. Model.*, **39**, 2489-2508.

Polit, O., Anant, C., Anirudh, B. and Ganapathi, M. (2018), "Functionally graded graphene reinforced porous nanocomposite curved beams: Bending and elastic stability using a higher-order model with thickness stretch effect", *Compos. Part B: Eng.* [In press]

Quan, T.Q., Tran, P., Tuan, N.D. and Duc, N.D. (2015), "Nonlinear dynamic analysis and vibration of shear deformable eccentrically stiffened S-FGM cylindrical panels with metal-ceramic-metal layers resting on elastic foundations", *Compos. Struct.*, **126**, 16-33.

Reddy, J.N. (2002), *Mechanics of Laminated Composite Concrete Plates and Shells: Theory and Analysis*, (Second Edition), CRC Press.

Rout, M., Hot, S.S. and Karmakar, A. (2019), "Thermoelastic free vibration response of graphene reinforced laminated composite shells", *Eng. Struct.*, **178**, 179-190

Shokravi, M. (2017), "Buckling of sandwich plates with FG-CNT-reinforced layers resting on orthotropic elastic medium using Reddy plate theory", *Steel Compos. Struct.*, *Int. J.*, **23**, 623-631.

Suman, S.D., Hirwani, C.K., Chaturvedi, A. and Panda, S.K. (2017), "Effect of magnetostrictive material layer on the stress and deformation behaviour of laminated structure", *IOP Conference Series: Materials Science and Engineering*, **178**(1), 012026.

Thai, H. and Vo, T. (2013), "A new sinusoidal shear deformation theory for bending, buckling and vibration of functionally graded concrete plates", *Appl. Math. Model.*, **37**, 3269-3281.

Thai, H., Park, M. and Choi, D. (2013), "A simple refined theory for bending, buckling, and vibration of thick concrete plates resting on elastic foundation, *Int. J. Mech. Sci.*, **73**, 40-52.

Thu, P.V. and Duc, N.D. (2016), "Nonlinear dynamic response and vibration of an imperfect three-phase laminated nanocomposite cylindrical panel resting on elastic foundations in thermal environments", *J. Sci. Eng. Compos. Mat.*, **24**(6), 951-962. DOI: 10.1515/secm-2015-0467

Vuong, P.M. and Duc, N.D. (2018), "Nonlinear response and buckling analysis of eccentrically stiffened FGM toroidal shell segments in thermal environment", *Aerosp. Sci. Technol.*, **79**, 383-398.

Wang, Y., Feng, Ch., Zhao, Zh. and Yang, J. (2018), "Eigenvalue buckling of functionally graded cylindrical shells reinforced with graphene concrete platelets (GPL)", *Compos. Struct.*, **20**, 238-246.

CC